

# A Family of Leukemia Inhibitory Factor-Binding Peptides that Can Act as Antagonists When Conjugated to Poly(ethylene glycol)<sup>†</sup>

W. Douglas Fairlie,<sup>‡,§,||</sup> Alessandro D. Uboldi,<sup>‡,§,||</sup> George J. Hemmings,<sup>§,||</sup> Brian J. Smith,<sup>§</sup> Helene M. Martin,<sup>§,||</sup> Phillip O. Morgan,<sup>§,||</sup> and Manuel Baca<sup>\*,§,||</sup>

The Walter and Eliza Hall Institute of Medical Research and The Cooperative Research Centre for Cellular Growth Factors, Parkville, Victoria 3050, Australia

Received July 23, 2003; Revised Manuscript Received September 15, 2003

**ABSTRACT:** A panel of six naïve 14-residue random peptide libraries displayed polyvalently on M13 phage was pooled and sorted against human leukemia inhibitory factor (LIF). After four rounds of selection, a single large family of peptides with the consensus sequence XCXXXXG(A/S)(D/E)(W/F)WXC<sub>F</sub> was found to bind specifically to LIF. Peptides within this family did not bind related members of the interleukin-6 family of cytokines, nor to murine LIF that has 80% sequence identity with human LIF. A representative peptide from this family was synthesized and found to bind to LIF with an affinity of approximately 300 nM. The phage-displayed form of this peptide was able to compete with the LIF receptor  $\alpha$  chain (LIFR) for binding to LIF; however, the free synthetic peptide was unable to inhibit LIF–LIFR binding or inhibit LIF bioactivity in vitro. Using a panel of human/murine chimeric LIF molecules, the peptide-binding site on LIF was mapped to a groove located between the B and the C helices of the LIF structure, which is distinct from the surfaces involved in binding to receptor. To mimic the effect of the phage particle and convert the free peptide into an antagonist of LIFR binding, a 40 kDa poly(ethylene glycol) (PEG) moiety was conjugated to the synthetic LIF-binding peptide. This PEG–peptide conjugate was found to be both an antagonist of LIF–LIFR binding and of LIF signaling in engineered Ba/F3 cells expressing LIFR and the gp130 coreceptor.

Leukemia inhibitory factor (LIF)<sup>1</sup> is a pleiotropic cytokine that is involved in the growth and differentiation of a range of cell types (1, 2). Some of these effects have been shown to be opposing in nature, depending on the cell type used. For example, one of the most common uses of LIF is to suppress the differentiation of murine embryonic stem cells in culture. In contrast, the standard assay used to measure LIF bioactivity is its ability to cause differentiation of murine myeloid M1 cells (2). LIF has a four-helical bundle structure (3, 4) and transduces its biological signal following ligand-induced heterodimerization of the LIF receptor  $\alpha$  chain (LIFR) and the gp130 coreceptor (5). The formation of the active signaling complex is a sequential process. LIF first binds to LIFR with nanomolar affinity, followed by subsequent binding of LIF–LIFR to gp130 to form the high

affinity (picomolar) signaling complex. The gp130 coreceptor is also used in the formation of signaling complexes by the structurally related cytokines interleukin (IL)-6, IL-11, oncostatin M (OSM), ciliary neurotrophic factor (CNTF), cardiotrophin-1 (CT-1), and cardiotrophin-like cytokine/cytokine-like factor-1 (CLC/CLF) (5). The shared use of a common coreceptor provides an explanation for the overlap in many of the in vitro functions of this family of proteins. However, while there is some redundancy in the functions of LIF, a number of its functions cannot be compensated for by other cytokines. Perhaps the best example of this is seen in female mice lacking the *LIF* gene (6). These animals were found to be infertile due to a failure in blastocyst implantation, and this phenotype could be rescued by the administration of purified recombinant LIF.

In contrast to *LIF*<sup>−/−</sup> mice, deletion of the *LIFR* gene gives a much more dramatic phenotype with animals dying perinatally with placental, skeletal, neural, and metabolic defects (7). This wide range of defects can be explained by the shared use of the LIFR by a subset of the cytokines that also utilize gp130, namely, LIF, OSM, CNTF, CT-1, and CLC/CLF. Hence, deletion of *LIFR* will affect the ability of these five cytokines to generate a biological signal.

Because of the critical role of LIF in murine fertility (6, 8), it is possible that antagonists of LIF signaling may act as contraceptive agents. Indeed, in two recent reports, the pregnancy rate of both monkeys and mice injected with neutralizing anti-LIF antibodies was significantly lower as compared to control animals (9, 10). As a consequence of

<sup>†</sup> The research was supported by a grant from The Contraceptive Research and Development (CONRAD) program (CIG-00-56) and the Cooperative Research Centres Program of the Australian Government. M.B. is the recipient of an Australian Research Fellowship from the Australian Research Council.

\* Corresponding author. E-mail: baca@wehi.edu.au.

<sup>‡</sup> These authors contributed equally to this work.

<sup>§</sup> The Walter and Eliza Hall Institute of Medical Research.

<sup>||</sup> The Cooperative Research Centre for Cellular Growth Factors.

<sup>1</sup> Abbreviations: ASP, active site point; CLC/CLF, cardiotrophin-like cytokine/cytokine-like factor-1; CNTF, ciliary neurotrophic factor; CT-1, cardiotrophin-1; ELISA, enzyme-linked immunosorbent assay; HRP, horseradish peroxidase; IL, interleukin; LIF, leukemia inhibitory factor; LIFR, leukemia inhibitory factor receptor  $\alpha$ -chain; LP, LIF-binding peptide; OSM, oncostatin M; PEG, poly(ethylene glycol); RP-HPLC, reverse-phase high-performance liquid chromatography; STAT, signal transducer and activator of transcription.

the shared use of LIFR and gp130 by several cytokines, specific antagonists of LIF signaling should ideally target LIF and not either of the two receptors. As a first step toward developing nonantibody-based antagonists of LIF signaling, we have panned phage-displayed peptide libraries in an effort to identify short peptides that can interact with LIF and block its receptor-binding activity. Phage display is now a commonly used technique for the identification of short peptides that can bind to target proteins (11). Although peptides are not normally considered good drug candidates, they can be readily synthesized, and given the difficulties in directly identifying small molecule antagonists of protein–protein interactions (12), they may provide an alternate route to low molecular weight antagonists through the design of peptide mimetics. In the present paper, we have used a set of phage-displayed libraries to identify a family of 14-residue peptides that bind to LIF with high affinity, high specificity, and when pegylated are capable of antagonising its activity *in vitro*.

## EXPERIMENTAL PROCEDURES

**Recombinant Proteins, Antibodies, and Peptides.** Neutra-vidin was purchased from Pierce Biotechnology, Inc. (Rockford, IL). Biotinylated LIF was prepared by treating LIF with 10 molar equiv of EZ-link sulfo-NHS-SS-biotin (Pierce, Rockford, IL) according to the manufacturer's instructions, followed by removal of excess reagent by gel filtration on a Bio-spin P6 column (Bio-Rad, Hercules, CA). Anti-human LIF monoclonal antibody MAB 250 was obtained from R & D Systems, Inc. (Minneapolis, MN), horseradish peroxidase (HRP)-conjugated anti-M13 phage antibody was from Amersham Biosciences (Uppsala, Sweden), anti-STAT3 polyclonal antibody sc-483 was from Santa Cruz Biotechnology (Santa Cruz, CA), and anti-phospho-STAT3 (Tyr 705) monoclonal antibody was from Cell Signaling Technology (Beverly, MA). HRP-conjugated sheep anti-rabbit Ig polyclonal antibody was purchased from Chemicon International (Temecula, CA).

LP-1 peptide (LCDGVVGAAWWECWQA) was prepared recombinantly as a C-terminal fusion to the SH2 domain derived from the protein tyrosine phosphatase SHP2, as described previously (13). A biotinylated analogue of the free LP-1 peptide (biotin-GGGDGLCDGVVGAAWWECWQ·amide) was chemically synthesized in-house using Fmoc chemistry as described previously (14). The crude peptide was oxidized (13) to form the intramolecular disulfide bond, prior to purification by reverse-phase HPLC (RP-HPLC). Peptide LP-1a (Ac-LCDGVVGAAWWECWQGGGK), also containing an intramolecular disulfide bond, was purchased from Auspep Pty. Ltd. (Melbourne, Australia).

LIFR cDNA corresponding to residues 52–536 of human LIFR, together with an N-terminal FLAG tag (DYKD-DDDK), was cloned into pCHO-1 vector (15), kindly provided by Dr. M. Tsuchiya (Chugai Pharmaceuticals, Japan). This extracellular region of human LIFR was then produced recombinantly in stably transfected Chinese hamster ovary cells. Concentrated supernatant containing the recombinant LIFR was loaded onto a lentil-lectin Sepharose 4B column (Amersham Biosciences, Uppsala, Sweden) and eluted with 0.3 M methyl- $\alpha$ -D-mannopyranoside. The eluate was then loaded onto M2 resin (Sigma-Aldrich, Sydney, Australia), washed with several column volumes of buffer

containing 100 mM NaCl, 20 mM Tris-Cl, pH 7.5, 0.02% (w/v) sodium azide, and eluted with 100  $\mu$ g/mL FLAG peptide in the same buffer. The M2 eluate was finally chromatographed on a Superdex 200 size-exclusion column using the same buffer as the previous step.

**Construction of Phage-Display Vectors and Libraries.** The in-house phagemid vector phg8\_4 was constructed for the production of M13 phage particles displaying short peptides fused to the amino terminus of the gene VIII protein (geneVIIIp). Briefly, the coding sequence for the mature gene VIII polypeptide was amplified by PCR from the M13 cloning vector M13mp18 and inserted between the *EcoNI* and the *EcoRI* sites in the expression vector pGEX-2T (Amersham Biosciences, Uppsala, Sweden). Sequential site-directed mutagenesis (16) was then used to replace a residual 17 base pair fragment upstream of gene VIII, coding for the first six amino acids of glutathione-S-transferase, with a PelB leader and linker sequence encoding the polypeptide sequence GGGTPTDPPTTPPTDSPGG, which is derived from *Streptomyces griseus* protease C (17). A *Kpn I* site was then inserted at the 5' end of the linker to facilitate excision of the linker-gene VIII coding sequence by *KpnI/EcoRI* digestion. A gene III display vector was also produced by replacing this linker-gene VIII fragment of the construct with a cDNA fragment of gene III protein (geneIIIp) encompassing codons 249–406.

Libraries of phage-displayed 14-residue peptides were prepared essentially as described by Sidhu et al. (18). The template vector used in making these libraries was a modified form of phg8\_4 in which the sequence GCCGACGGTTT-AATTAATTGACAATTAAATCTTAGATATATTTAAGT-TAACTAG was inserted between the PelB leader and polypeptide linker. Kunkel mutagenesis (16) was used to randomly mutate the underlined portion of this sequence, and transformation of a nonsuppressor strain of *Escherichia coli* (XL-1 Blue), followed by infection with M13KO7 helper phage (19), resulted in the production of phage particles displaying random sequence peptides with a fixed ADG-tripeptide motif at the N-terminus and fused at their C-terminus to geneVIIIp. Each library was initially propagated in 500 mL of 2YT medium containing 100  $\mu$ g/mL ampicillin and approximately  $10^{11}$  M13KO7 helper phage. Phagemid stocks were purified from culture supernatants by precipitation with a saline poly(ethylene glycol) solution and resuspended in 2 mL of phosphate-buffered saline (PBS) at a final concentration of approximately  $10^{14}$  phagemid/mL. An equal aliquot from each library was combined prior to panning the pooled libraries against LIF.

**Panning of Peptide Libraries Against Human LIF.** Phage from the pooled peptide library pool ( $\sim 10^{13}$  phagemid) and biotinylated LIF (100 nM final) were diluted to 1 mL in PBS containing 0.1% (v/v) Tween-20 (PBS/Tween) and 1% (w/v) skim milk powder. After incubating for 2 h at room temperature, streptavidin-coated magnetic beads (Promega, Madison, WI), which had been blocked with 6% (w/v) skim milk powder, were then added to the sample to capture the biotinylated LIF along with any associated phage particles. After 15 min incubation with gentle mixing, the beads were washed 10 times with PBS/Tween, followed by elution of bound LIF by cleavage of the disulfide-containing biotin linker using 75 mM DTT in 0.1 M Tris, pH 8.0. The eluted phage were repropagated by infection of *E. coli* and harvested

from an overnight culture in 50 mL of 2YT medium containing 100  $\mu\text{g/mL}$  ampicillin and approximately  $10^{10}$  M13KO7 helper phage. A second round of panning was performed using biotinylated LIF bound to neutravidin-coated polystyrene plates. Briefly, five wells of a Maxisorp 96-well microplate were coated overnight with neutravidin (20  $\mu\text{g/mL}$ ) in PBS. After blocking with PBS containing 6% (w/v) milk powder and washing, wells were incubated with 100  $\mu\text{L}$  of biotinylated LIF (20  $\mu\text{g/mL}$  in PBS/Tween) for 2 h before washing 15 times with PBS/Tween. Approximately  $10^{13}$  phagemid, repropagated after the first round of panning, were diluted into 100  $\mu\text{L}$  of PBS/Tween containing 1% (w/v) skim milk and added to the LIF-coated wells. After incubation for 1 h at room temperature, wells were washed with PBS/Tween, and LIF-bound phage were eluted by the addition of 75  $\mu\text{L}$ /well of 75 mM DTT in 25 mM Tris, pH 8.0 containing 0.1% (v/v) Tween-20. Eluted phage were repropagated as previously described, and a further two rounds of panning were performed by repeating the previous process.

**Screening and Sequencing of Clones.** After the final round of panning, eluted phage were serially diluted and used to infect XL-1 Blue *E. coli* for 1 h prior to plating overnight on agar. Individual colonies were picked and grown in 2YT for 8 h at 37 °C, and then M13KO7 helper phage and isoIPTG (10  $\mu\text{M}$  final concentration) were added prior to overnight incubation. Following centrifugation, 50  $\mu\text{L}$  of culture supernatant was used for analysis by ELISA. Clones that gave the highest specific response for binding to LIF (with low background binding) were then selected for sequencing.

To determine the sequences of peptides displayed by the selected clones, 1  $\mu\text{L}$  of culture supernatant was used in a PCR to amplify a fragment encompassing the encoded peptide sequence. This PCR product was then treated with ExoSAPit, (USB Corp., Cleveland, OH) to degrade unconsumed deoxynucleotides and primers, and sequenced directly.

**Construction of LIF Mutants.** To map the interaction site on LIF for the peptide, human/murine chimeric mutants of LIF were made by site-directed mutagenesis using the method of Kunkel et al. (16). These mutants were displayed on phage as fusions to the geneIIIp.

**Enzyme-Linked Immunosorbent Assay (ELISA).** Prior to analysis of peptide-binding affinities by phage ELISA, peptides of interest were displayed as gene III fusions following replacement of the *KpnI/EcoRI* fragment of the gene VIII display construct with the corresponding fragment from the gene III display vector. Competitive phage ELISAs were performed essentially as described previously (13), where LIF or peptide in solution were used to displace phage-displayed peptide from binding to immobilized LIF. For experiments in which the peptide-binding site was mapped, biotinylated LP-1 peptide (0.5  $\mu\text{g/mL}$ ) was immobilized onto plates initially coated with 10  $\mu\text{g/mL}$  streptavidin. Serial dilutions of human/murine chimeric LIF mutants, displayed as fusions to geneIIIp on the surface of phage, were added in 100  $\mu\text{L}$  of 1% (w/v) skim milk in PBS and incubated for 2 h. After washing, bound phage particles were labeled with anti-M13 polyclonal antibody-HRP conjugate and assayed.

**Pegylation of Peptide.** Peptide LP-1a (2 mg; 0.97  $\mu\text{mol}$ ) was dissolved in 0.5 mL of 100 mM sodium phosphate buffer (pH 8.0) containing 20 mg (0.5  $\mu\text{mol}$ ) of poly(ethylene

Table 1: Naïve Peptide Library Designs<sup>a</sup>

library	design
1	X <sub>14</sub>
2	CX <sub>12</sub> C
3	XCX <sub>10</sub> CX
4	X <sub>2</sub> CX <sub>8</sub> CX <sub>2</sub>
5	X <sub>3</sub> CX <sub>6</sub> CX <sub>3</sub>
6	X <sub>4</sub> CX <sub>4</sub> CX <sub>4</sub>

<sup>a</sup> Libraries were all displayed as fusions to the gene VIII coat protein. The position of the fixed cysteines in libraries 2–5 are indicated, and X indicates the randomized amino acids in each library encoded by an NNS codon.

glycol) (40 kDa)-NHS (PEG-NHS) (Shearwater Polymers Inc., Huntsville, AL). Following overnight incubation at room temperature, the pegylated peptide was purified by RP-HPLC on a 25 × 0.7 cm C4 column (incubated at 50 °C) with a 30 min gradient of 0–60% (v/v) acetonitrile in 0.1% (v/v) trifluoroacetic acid. Following lyophilization of the product-containing fractions, 7.4 mg of peptide–PEG conjugate was obtained.

**STAT-3 Tyrosine Phosphorylation Assay.** Ba/F3 cells ( $5 \times 10^6$  cells/sample) stably transfected with human LIFR and gp130 were grown in serum- and IL-3-free medium for 3 h prior to stimulation with 10 ng/mL LIF that had been preincubated for 1 h with either medium alone or medium containing either LP-1a, pegylated LP-1a, or unconjugated PEG derived from a stock solution that had been incubated overnight in PBS buffer to hydrolyze the NHS group. After 20 min at room temperature, cells were lysed for 30 min at 4 °C in RIPA buffer (50 mM Tris pH 8.0, 150 mM NaCl, 0.5% (w/v) sodium deoxycholate, 1% (v/v) Nonidet P-40, 0.1% (w/v) SDS), supplemented with complete protease inhibitor cocktail (Roche Applied Science), 1 mM Na<sub>3</sub>VO<sub>4</sub>, 1 mM NaF, and 1 mM phenylmethylsulfonylfluoride. Following centrifugation to remove cell debris, 20  $\mu\text{L}$  of the lysate was subjected to SDS–PAGE on a 7.5% acrylamide gel and then transferred to a PVDF membrane. After blocking, the membrane was probed with either an anti-STAT3 polyclonal or an anti-phospho-STAT3 (Tyr 705) monoclonal antibody. After incubation with HRP-conjugated anti-rabbit immunoglobulin polyclonal antibody, proteins were visualized using chemiluminescence reagents (Pierce, Rockville, IL).

## RESULTS

**LIF-Specific Peptides from Phage-Displayed Libraries.** To identify peptides that bound specifically to human LIF, a series of phage-displayed peptide libraries was prepared and panned against recombinant human LIF. A total of six peptide libraries were prepared, with one library containing 14 random residues, while the remaining five libraries contained 12 random residues in the context of a fixed length disulfide-constrained loop (Table 1). These peptides were displayed polyvalently on gene VIII to enable the selection of peptides with a wide range of affinities via avidity effects (18). The molecular diversity of each of these libraries was estimated to range between  $10^9$  and  $10^{10}$  unique peptide sequences.

To streamline the panning process, a single library pool was used in which the six random peptide libraries were combined. This library pool was panned against biotinylated

Table 2: Human LIF-Binding Sequences Selected from Naïve Libraries<sup>a</sup>

PEPTIDE SEQUENCES											IC <sub>50</sub> (nM)			
1	5					10								
L	C	D	G	V	V	G	A	A	W	W	E	C	W	25
L	C	E	T	L	S	G	S	L	W	W	E	C	F	39
D	C	W	Q	S	F	G	M	D	F	W	L	C	Y	17
L	C	Q	S	F	Q	G	S	E	W	W	M	C	F	34
Y	C	G	S	K	E	P	F	M	W	W	L	C	F	39
S	C	V	S	L	S	G	A	E	W	W	S	C	W	25
W	C	A	G	F	G	G	A	D	W	W	D	C	F	-
N	C	W	N	S	L	G	S	E	F	W	L	C	I	-
W	C	G	D	L	L	G	S	Q	F	W	D	C	Y	-
F	C	E	E	L	S	G	V	A	W	W	W	C	F	-
P	C	D	L	F	A	G	S	E	W	W	L	C	L	-
F	C	E	G	K	E	A	W	E	W	W	L	C	F	-
L	C	D	W	A	K	G	A	D	W	W	L	C	F	-
L	C	D	L	L	V	G	A	E	W	W	S	C	W	-
L	C	D	S	L	L	G	D	W	W	L	C	C	L	-
W	C	E	R	M	E	A	W	Q	W	W	L	C	F	-
F	C	W	G	V	M	G	A	E	W	W	E	C	W	-
W	C	W	E	L	R	E	T	A	F	W	E	C	F	-
A	C	W	E	L	E	G	W	L	F	W	E	C	F	-
S	C	E	M	I	W	G	S	D	W	W	L	C	F	-
W	C	P	G	L	S	G	V	E	W	W	V	C	F	-
L	C	T	M	A	Y	G	S	E	W	W	W	C	M	-
W	C	D	W	V	V	G	A	E	Y	W	V	C	M	-
A	C	A	G	L	R	G	V	E	W	W	W	C	F	-
M	C	G	L	R	W	G	A	D	W	W	A	C	F	-

<sup>a</sup> The sequences shown are from 24 representative LIF-binding clones sequenced following four rounds of sorting. The boxes indicate the cysteine residues that were fixed within each peptide sequence during library construction. The IC<sub>50</sub> values were determined for a representative selection of peptide sequences by a competition ELISA using immobilized LIF with the peptide displayed as a gene III fusion on phage and various concentrations of LIF in solution.

LIF, using alternate rounds of panning with LIF in solution and LIF bound to neutravidin coated on polystyrene plates. The use of these two panning strategies minimized the risk of selecting peptides that would bind to agents other than LIF. After four rounds of panning, 96 individual phage clones were propagated and compared for binding to LIF directly immobilized on polystyrene plates versus binding to a mixture of streptavidin/neutravidin. All of the selected clones showed strong binding to LIF but not streptavidin/neutravidin. A number of these clones were then selected at random for sequencing of the encoded peptide insert. From this analysis, a family of homologous peptides emerged that were derived from the XCX<sub>10</sub>CX sublibrary (Table 2). The consensus sequence for these LIF-binding peptides contained a glycine residue at position 7 and usually a tryptophan or in some cases another residue with a bulky, hydrophobic side chain at positions 10, 11, and 14. A weaker preference for a hydrophobic residue at position 1, an alanine or serine at position 8, and an acidic residue (aspartic or glutamic acid) at position 9 was also observed.

**Affinity and Specificity of LIF-Binding Peptides.** Because of the large number of related LIF-binding peptide sequences obtained, a subset of representative peptides was selected for further analysis. These peptides were subcloned into a gene III phage-display vector, and the LIF-binding affinities were determined in a competition phage ELISA. All of the peptide sequences behaved similarly with IC<sub>50</sub> values in the range of 17–39 nM (Table 2). A peptide corresponding to one of these clones (LP1: LCDGVVGAAWWECWQA) was

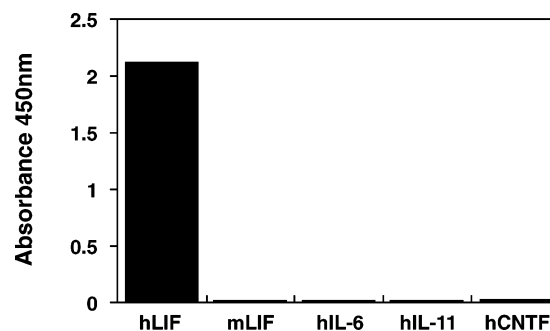


FIGURE 1: LIF-binding peptide LP-1 binds specifically to human LIF. The LIF-binding peptide LP-1 was tested for its ability to bind to various LIF-related proteins in an ELISA. Proteins were coated onto polystyrene plates at 5  $\mu$ g/mL and then incubated with a fixed dilution of phage displaying the LP-1 sequence as a fusion to the gene III coat protein.

prepared recombinantly as a C-terminal fusion to the SH2 domain from SHP2 (13) and tested for its ability to compete with the same peptide displayed on phage for binding to LIF. The IC<sub>50</sub> for this competition was 1.0  $\mu$ M (i.e., approximately 40-fold weaker in this assay than if soluble LIF was used as the competitor instead of the LP-1 peptide fusion). A chemically synthesized analogue of the free LP-1 peptide (biotin-GGGDGLCDGVVGAAWWECWQ·amide) also gave a similar IC<sub>50</sub> (300 nM) in this assay, indicating that the affinity differences observed were not due to the protein fusion partner. We believe that the difference in the apparent affinities of LIF binding to the free versus phage-displayed peptide may be the result of avidity effects due to more than a single copy of the geneIIIp-peptide fusion being displayed on each phage particle. Alternatively, residues in the linker region between peptide and geneIIIp, which are not present in the synthetic peptide, may also be contributing to the interaction. Interestingly, the recombinant and synthetic LP-1 peptides included a glutamine residue at the C-terminus corresponding to the first residue of the linker connecting the peptide to geneIIIp or geneVIIIp in the phage-displayed form of the peptide. When an alternate fusion construct was recombinantly prepared without this glutamine residue (LCDGVVGAAWWECW), a further 70-fold decrease in binding affinity was observed (IC<sub>50</sub> = 70  $\mu$ M) (data not shown), suggesting that this part of the linker region of the phage-displayed peptide did indeed contribute to the association with LIF.

To assess the specificity of the binding interaction of LP-1 for LIF, the phage-displayed peptide was tested in an ELISA for its ability to bind to murine LIF as well as the related proteins IL-6, IL-11, and CNTF. No binding was observed to any of these other proteins (Figure 1). This indicates that the peptide is highly specific for binding to human LIF, particularly given the lack of binding to murine LIF that is approximately 80% identical to human LIF (141/180 residues identical).

**Inhibition of the LIF–LIFR Interaction by a LIF-Binding Peptide.** To determine whether the LIF-binding peptide LP-1 could antagonize the interaction between LIF and LIFR, a competition ELISA was performed in which soluble LIFR

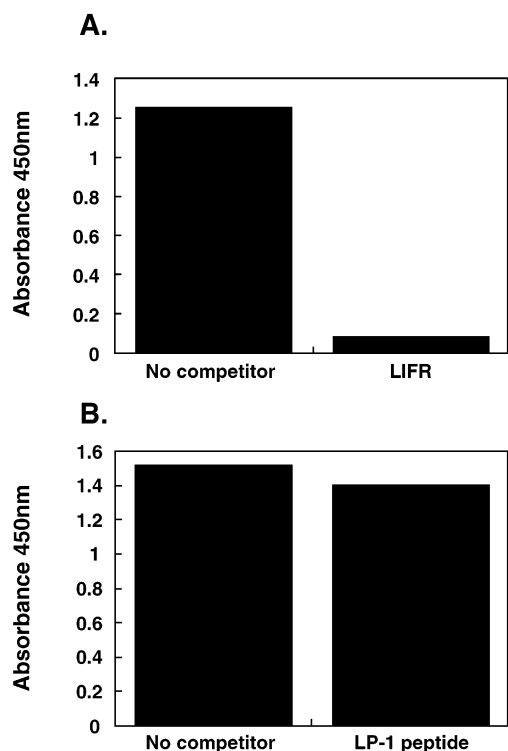


FIGURE 2: LIF-binding peptide LP-1 cannot inhibit interaction of LIF-LIF-R. Competition ELISAs were performed to determine whether the LP-1 peptide sequence could act as an antagonist of the LIF-LIFR interaction. The assays were performed in two different formats. (A) LIF was coated onto a plate at 5  $\mu\text{g/mL}$  and then incubated with phage displaying the LP-1 sequence as a geneIIIp fusion in the presence or absence of 500 nM LIFR. Bound phage were detected using a HRP-conjugated anti-M13 phage antibody. (B) Plates were coated with 2.5  $\mu\text{g/mL}$  LIFR and incubated with 50 pM recombinant LIF in the presence or absence of 65  $\mu\text{M}$  synthetic peptide, LP-1. The anti-LIF monoclonal antibody MAB 250 (2  $\mu\text{g/mL}$ ) was then used to detect receptor-bound LIF.

was tested for its ability to compete with phage-displayed LP-1 for binding to LIF. In these experiments, inhibition of binding of phage-displayed LP-1 to immobilized LIF was observed, which suggested that the LP-1 sequence might be able to act as an antagonist of LIFR binding.

However, when the soluble forms of peptide LP-1, either as free synthetic peptide (Figure 2B) or as the recombinant fusion product (data not shown), were tested for their ability to inhibit the LIF-LIFR interaction, no inhibition was observed, even at concentrations up to 65  $\mu\text{M}$ . We thought that the initial result with the phage-displayed form of the peptide was likely to be a consequence of steric effects that result from the peptide being associated with the large phage particle. Hence, we concluded from the results of the assays using the free (i.e., nonphage-displayed) peptide that LP-1 is not an antagonist of the LIF-LIFR interaction.

**Pegylated LP-1 Derivative Is an Antagonist of LIFR Binding and LIF Bioactivity.** The phage-displayed form but not free LP-1 peptide appeared to act as an antagonist of the LIF-LIFR interaction. To determine whether this was due to steric hindrance, we attempted to mimic the effect of the phage particle, and hence the antagonism, by conjugating the LIF-binding peptide to a large polymeric molecule. We therefore coupled a 40 kDa poly(ethylene glycol) derivative to the LIF-binding peptide to see if this conjugate could act

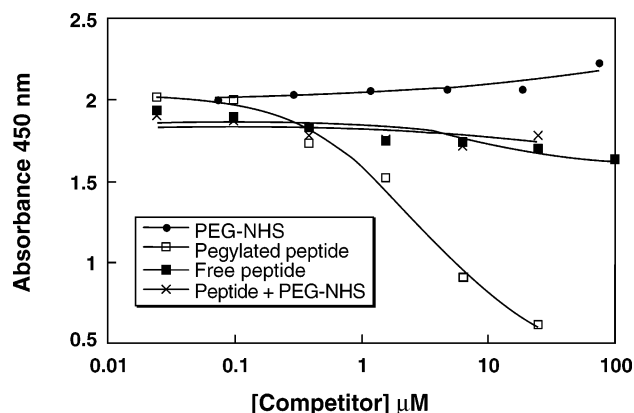


FIGURE 3: Pegylated LIF-binding peptide can inhibit binding of LIF to LIFR. The ability of pegylated LP-1a to inhibit binding of LIF to LIFR was determined by competition ELISA. Plates were coated with LIF-R and then incubated with LIF displayed on phage as a geneIIIp fusion with various concentrations of either pegylated peptide LP-1a, unconjugated peptide LP-1a, free PEG-NHS that had been hydrolyzed, or 1:1 unconjugated peptide + hydrolyzed PEG-NHS. Binding of phage to LIFR was determined using an HRP-conjugated anti-M13 antibody.

as an antagonist of LIF-LIFR binding. For these experiments, the LP-1 sequence was resynthesized (LP-1a: Ac-LCDGVVGAAWWECWQGGGK) with an acetylated N-terminus and C-terminal lysine residue separated by a glycine spacer. This enabled specific attachment of the NHS-derivatized PEG molecule to the lysine side chain, thus mimicking the mode of attachment of LP-1 to the phage particle through the C-terminus.

The purified LP-1a-PEG conjugate was tested in a competition ELISA to determine whether it could antagonize binding of phage-displayed LIF to the LIFR. A concentration dependent inhibition of LIF binding was observed, with an  $\text{IC}_{50}$  of 3  $\mu\text{M}$ . By contrast, no inhibition was observed for the unconjugated peptide, free PEG, or a combination of both (Figure 3).

Both the pegylated peptide conjugate and the unconjugated peptide were also tested in a cell-based assay to determine whether they could act as antagonists of LIF bioactivity in vitro. Although the unconjugated peptide was unable to inhibit the interaction of LIF with LIFR, it was possible that it may be able to inhibit the interaction with gp130 and hence still inhibit LIF bioactivity. For this assay, we examined the ability of the peptides to inhibit LIF-induced tyrosine phosphorylation of the latent transcription factor signal transducer and activator of transcription 3 (STAT3) in Ba/F3 cells stably expressing human LIFR and gp130. Phosphorylation of STAT3 is a key step in the signal transduction pathway downstream of LIFR/gp130 receptor activation and has been previously used to measure the effects of LIF antagonists (20).

Following stimulation of the engineered Ba/F3 cell line with LIF, phospho-STAT3 could be readily detected by Western blotting analysis of cell lysates (Figure 4). By contrast, no STAT3 phosphorylation was detected for unstimulated cells. When the cells were stimulated with LIF in the presence of the unconjugated peptide LP-1a at a concentration of 100  $\mu\text{M}$ , no inhibition of STAT3 phosphorylation was apparent, further confirming that the free peptide is unable to inhibit the LIF-LIFR interaction and also demonstrating that the peptide does not interfere with gp130

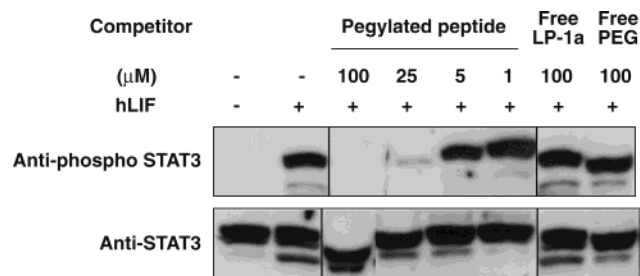


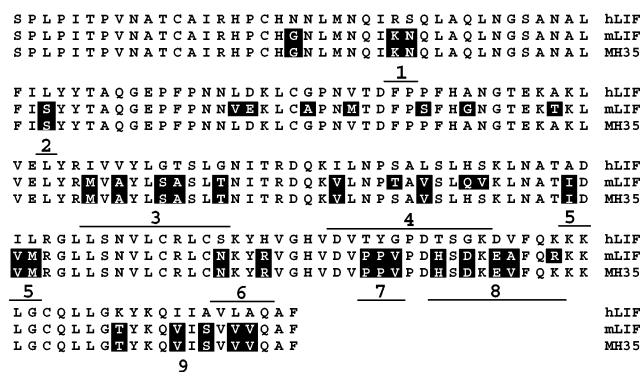
FIGURE 4: Pegylated LIF-binding peptide can inhibit LIF-induced STAT3 phosphorylation. Ba/F3 cells expressing LIFR and gp130 were incubated either without (–) LIF or with (+) LIF (10 ng/mL) that had been preincubated for 1 h prior to addition with either medium alone, pegylated peptide LP-1a, unconjugated LP-1a, or free PEG at the indicated concentrations. After the cells were lysed, the lysates were separated by SDS–PAGE on 7.5% gels and immunoblotted with either an anti-phospho STAT3 monoclonal antibody or an anti-STAT3 polyclonal antibody as a loading control.

binding. The pegylated form of the peptide, however, was able to inhibit LIF-induced STAT3 phosphorylation in a concentration dependent fashion. Complete inhibition was observed at a concentration of 100  $\mu$ M peptide conjugate and almost complete inhibition at 25  $\mu$ M. At concentrations of 5  $\mu$ M and less, no apparent inhibition of STAT3 phosphorylation was detected, demonstrating that the peptide conjugate must be at a concentration in excess of its  $IC_{50}$  for inhibiting LIFR binding to be effective as an antagonist of LIF signaling. As expected, the unconjugated PEG reagent had no detectable effect on STAT3 phosphorylation at a concentration of 100  $\mu$ M.

**Mapping the LP-1-Binding Site.** Because of the high specificity of LP-1 for binding to human LIF, the submicromolar affinity of the interaction, and the ability of the pegylated conjugate to act as an antagonist, we thought it would be of value to map the binding site on LIF for the peptide. These experiments made use of the observation that the LIF-binding peptides did not display detectable binding to murine LIF (Figure 1), nor to a murine/human chimeric LIF known as MH35 (21), which differs from human LIF by only 27/180 residues (data not shown). We therefore divided the residues that differed between the human and the murine LIF into nine clusters and mutated the human sequence within each cluster to the corresponding murine sequence (Figure 5A). Rather than express soluble protein for each of the human/murine chimeras, we devised a simple ELISA assay using the phage-displayed proteins. In this assay, each human/murine chimera was expressed monovalently as a geneIIIp fusion and titrated against a biotinylated form of LP-1 captured on streptavidin-coated microtiter plates. Each phage-displayed LIF mutant was also titrated against immobilized LIFR as a control for any differences in the level of functional protein display. The ratio of peptide versus LIFR binding was calculated for each human/murine LIF chimera and normalized against the same ratio obtained for wild-type human LIF (Figure 5B). Using this strategy, high peptide/LIFR-binding ratios, relative to wild-type LIF, indicate an effect of the mutation on peptide binding.

When analyzed in this way, mutants 1, 2, 6, 7, and 9 gave peptide/LIFR-binding ratios that were similar to wild-type LIF, indicating no apparent effect on peptide binding. Mutants 3 and 5 gave peptide/LIFR-binding ratios that were significantly higher than wild-type LIF, suggesting these

## A.



## B.

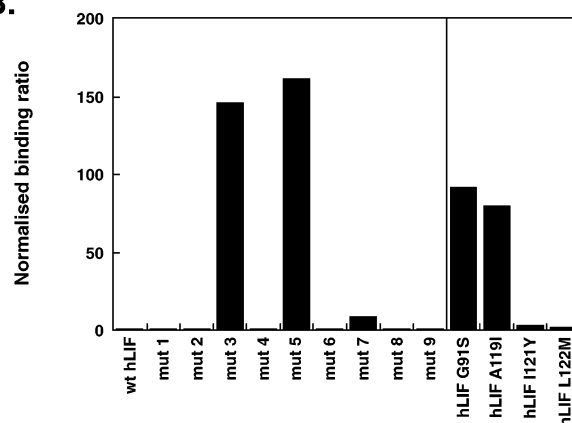


FIGURE 5: Binding site on LIF for the LIF-binding peptide LP-1 involves residues on helices B and C. The binding site on LIF for the LIF-binding peptide was determined using human/murine LIF chimeras. (A) Nine mutants of human LIF (hLIF) were made in which residues were substituted with the corresponding residues from murine LIF (mLIF) and displayed on phage as fusions to the geneIIIp coat protein. As the peptide did not bind to the human/murine chimera known as MH35, only those regions of hLIF that differed in sequence to MH35 were mutated. (B) Phage-displayed human LIF and each of the nine LIF mutants were assessed in an ELISA assay for their ability to bind to immobilized LIF-binding peptide LP-1, as well as to immobilized LIFR or an anti-LIF monoclonal antibody. Phage were titrated against peptide, LIFR, and antibody, and the dilution of phage that gave a half-maximal response ( $EC_{50}$ ) was calculated. The normalized binding ratios were calculated by dividing the  $EC_{50}$  for peptide binding by the  $EC_{50}$  for LIFR binding (mutants 1–3, 5–7, and 9) or antibody binding (mutants 4 and 8) and dividing these values by the same ratio obtained for wild-type human LIF. Several point mutations were made to confirm the location of the binding site, and then the peptide/LIFR-binding ratios were determined as described.

mutants had a greatly reduced affinity for binding the peptide. In the case of mutants 4 and 8, the peptide/LIFR-binding ratios were significantly lower than for wild-type LIF, suggesting that some of the mutations introduced may have effected the interaction with LIFR. Therefore, to reassess the relative binding of these mutants to the peptide, the assay was repeated using an anti-LIF monoclonal antibody instead of LIFR for normalization. In this assay, peptide/antibody-binding ratios within 2-fold that of wild-type LIF were obtained for mutants 4 and 8, indicating that there was no major effect of the mutations in these proteins on peptide binding.

Mutants 3 and 5 had showed significantly reduced peptide binding following correction for LIFR binding (Figure 5B).

The nonhuman sequence in mutant 3 is located on helix B, while that in mutant 5 is located on helix C. When mapped onto the three-dimensional structure of LIF, the helix C substitutions in mutant 5 (A119I, I121V, and L122M) were found to be in close proximity to G91, a helix B residue replaced in mutant 3. To determine whether this cluster of residues was important for peptide binding, each of these four residues in human LIF was individually mutated to the corresponding murine amino acid and reassessed for peptide and LIFR binding. Of these point mutants (G91S, A119I, I121V, and L122M), a significant increase in the peptide/LIFR-binding ratio was observed for the G91S and A119I mutants (Figure 5B). These combined results suggest that at least part of the peptide-binding epitope is located on the B and C helices of LIF in the vicinity of residues G91 and A119.

**Peptide-Binding Site Corresponds to a Potential Small Molecule-Binding Pocket.** Examination of the three-dimensional structure for human LIF indicated the presence of a well-defined groove or pocket on LIF in the region of Gly91/Ala119. A similar pocket was not apparent in the equivalent region on the murine LIF structure (4) or the structure of the MH35 chimeric LIF (3). This difference in the structures suggested a basis for the species specificity of the LIF-binding peptides. To further compare the surface characteristics of human versus murine LIF, the PASS program (putative active sites with spheres) was used to identify surface cavities on either structure (22).

The PASS program (22) is used for the determination of likely positions of ligand-binding sites on a protein surface by identifying cavities or crevices large enough to accommodate a ligand and that possess a substantial solvent excluded volume. The algorithm itself involves coating the surface of the protein with sets of probe spheres, retaining those with low solvent accessibility and identifying some of these as likely centers of binding pockets. When applied to human and murine LIF (Figure 6), the PASS program identified a large pocket on the surface of human LIF in the vicinity of Gly91/Ala119, with an estimated volume of 295 Å<sup>3</sup> (Figure 6A). In comparison, no similar pocket on the surface of murine LIF was identified in this region (Figure 6B). The pocket identified on human LIF in the region around Gly91/Ala119 was the largest such site on the entire protein indicating this to be a potential site where ligands might interact.

## DISCUSSION

In this paper, we describe the discovery, using phage-displayed random peptide libraries, of a family of 14-residue peptides that were highly specific for human LIF. Although the phage-displayed form of the peptide was able to inhibit the binding of LIFR to LIF, the free peptide did not have this activity, nor was it able to inhibit LIF bioactivity in vitro. Using interspecies LIF chimeras, we were able to map a binding site for this family of peptides to an area located on the B and C helices of LIF. In particular, the region in the vicinity of residues Gly91 and Ala119 appeared to be important for the interaction. The location of this peptide-binding site is consistent with the inability of the free peptide to act as a LIF antagonist. Residues critical for binding to LIFR (i.e., Lys156 and Phe159), as determined by Hudson et al.

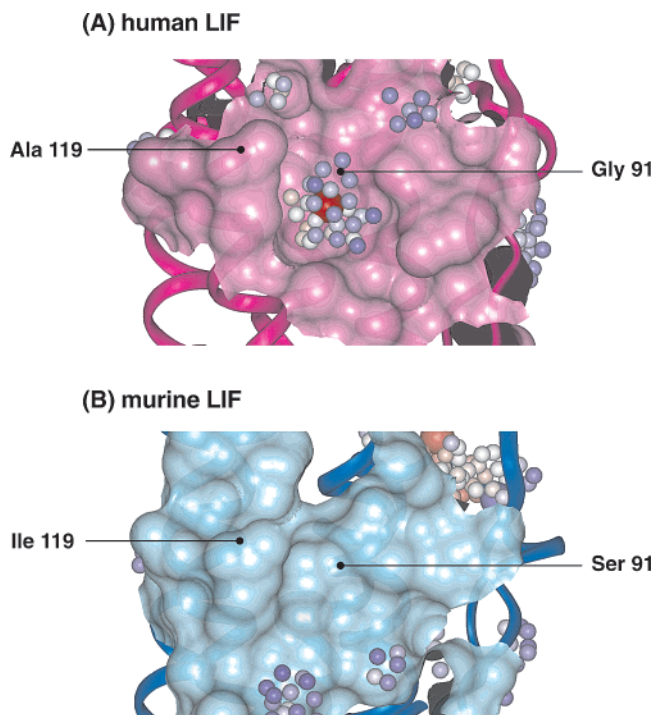


FIGURE 6: Identification of potential ligand-binding sites using PASS. Partial molecular surfaces of (A) human and (B) mouse LIF in the vicinity of Gly91 and Ala119 are shown. Structures were obtained from the PDB accession codes 1EMR and 1LKI (4). PASS probes are shown as small spheres, color coded from red through white to blue, indicating the extent of burial of the probes from high to low burial. Larger spheres that indicate active site points (ASP) are color coded from red through white to blue indicating the probe weight. The ASPs identify central probes in a cluster of probes, while the probe weight is proportional to the number of probes in the vicinity of the ASP and the extent to which the probes are buried. The figure was generated using the InsightII package (Accelrys, San Diego).

(23), are located at the top of the four-helix bundle (i.e., well away from the peptide-binding site in the view shown in Figure 7). The binding site for gp130 is also nonoverlapping, although it is somewhat closer to the peptide-binding site and involves residues on helices A (Gln25, Ser28, and Gln32) and C (Asp120, Ile121, Gly124, and Ser127) (23).

As the peptides identified bound LIF with reasonable affinity ( $\sim 1 \mu\text{M}$ ), we did not attempt to isolate higher affinity mutants by screening partially randomized libraries. However, the large variability observed in the amino acid sequence at nonconserved positions within the LIF-binding peptides (Table 2), together with the similar binding affinities displayed by a subset of these, suggests that randomization of nonconserved positions may not necessarily lead to optimized variants with significantly enhanced affinity. Given the apparent involvement of the C-terminus in binding, though, it may be possible to identify higher affinity mutants by screening a library containing a randomized C-terminal tail beyond the LIF-binding consensus motif. Alternatively, structural characterization of the peptide–LIF complex could provide valuable insights into how the binding affinity of the complex could be improved, such as by rational design of modified peptide analogues or by guiding the design of secondary peptide libraries based on the LIF-binding consensus sequence.

The ability of the phage-displayed form of the LIF-binding peptide to act as a receptor-binding antagonist was most

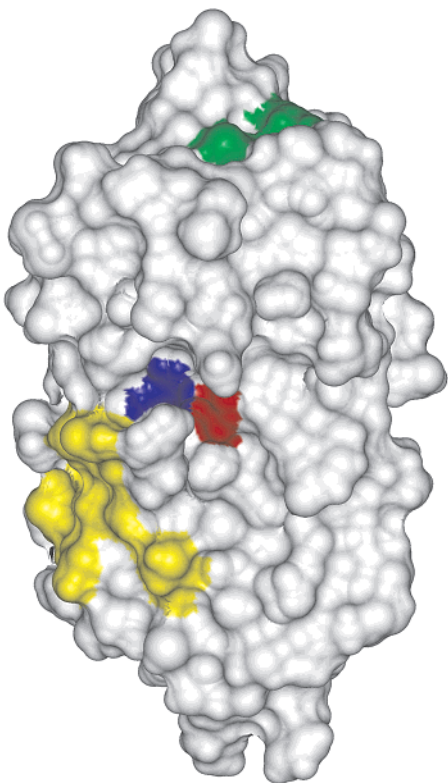


FIGURE 7: Residues on LIF involved in binding to LP-1 are spatially distinct from the LIFR- and gp130-binding sites. Molecular surface of human LIF (PDB code 1EMR) with residues important for interaction with the LIF-binding peptides; Gly91 and Ala119 are shown in red and blue, respectively. Residues previously determined (23) to be important for interaction of LIF with LIFR (Phe156 and Lys159) are shown in green and with gp130 (Gln25, Ser28, Gln30, Asp120, Ile121, Gly124, and Ser127) in yellow. The figure was generated using the InsightII package (Accelrys, San Diego).

likely a consequence of the bulky phage particle masking the receptor-binding epitope on LIF. We were able to mimic this effect by coupling the peptide to a large polymer molecule. A conjugate of peptide and poly(ethylene glycol) was found to be an antagonist of LIFR binding and of LIF bioactivity. The long extended nature of the poly(ethylene glycol) polymer appeared to be important for the antagonist activity, as neither C- nor N-terminal fusions of the peptide to the globular 15 kDa SH2 domain from SHP2 produced an antagonist of LIFR binding or LIF bioactivity (data not shown). While conjugation of poly(ethylene glycol) to the peptide was important for converting the peptide into an antagonist, it can be also advantageous if peptides are to be used for in vivo studies. Poly(ethylene glycol) is known to modify the pharmacokinetic properties of peptides, notably by increasing the circulatory half-life as well as improving their solubility (24). Hence, the pegylated LIF antagonist peptides may be suitable for in vivo testing in animals, although the selection of higher affinity mutants would be desirable prior to such studies.

Comparison of the molecular surface of human LIF, in the vicinity of the peptide-binding site, to the corresponding region on murine LIF provides some insight as to why the peptides were unable to bind to murine LIF. In the human protein, a groove or pocket exists between residue Gly91 on the B helix and Ala119 on the C helix. This groove is essentially absent in murine LIF, primarily due to the

substitution of Gly91 and Ala119 with serine and isoleucine, the side chains of which occupy the space corresponding to the groove in human LIF. Interestingly, this pocket was identified, by the PASS program, as the most likely site on human LIF into which a small ligand might bind. Thus, the LIF-binding peptide is targeting a potential small molecule-binding site on LIF. This contrasts with other protein-binding peptides discovered by phage display, which often target flat protein surfaces and bury large surface areas in the peptide–protein complexes (25). Moreover, peptide ligands against these flat protein surfaces often act as antagonists of protein–protein interactions, while the LIF-binding peptide, which appears to be targeting a small, well-defined pocket, does not act an antagonist of LIF receptor binding. Although a structure of the peptide–LIF complex would be required to reveal whether the peptide contacts LIF only within this pocket or at other additional sites, it is tempting to speculate that the peptide has identified a binding site on the surface of LIF that could accommodate a small molecule ligand.

Short peptides have the potential to be translated into small organic molecules and hence provide lead compounds for the design of drugs that can be administered orally. This has been difficult to do for peptides identified from phage-display libraries that target extracellular proteins, as many of these bind the target protein using an extended interface that is difficult to mimic with a small molecule (25). The LIF-binding peptides described here may be more amenable to small molecule mimicry based on their specific interaction with a pocket on the surface of human LIF. Although small molecule mimics of these peptides are unlikely to be antagonists of LIF signaling, they may represent a useful model system for developing methods to discover small molecule ligands of proteins either by mimicry of the peptide or by screening libraries of small molecules to identify compounds that can compete with the peptide for binding to LIF.

## ACKNOWLEDGMENT

We thank Joanne McCoubrie, Wendy Carter, and David De Souza for technical assistance; AMRAD Corp. Australia for providing the LIF; and Dr. Richard Simpson for IL-6 and Dr. Lorraine Robb for the IL-11 used in these studies.

## REFERENCES

1. Metcalf, D. (1992) *Growth Factors* 7, 169–173.
2. Hilton, D. J. (1992) *Trends Biochem. Sci.* 17, 72–76.
3. Hinds, M. G., Maurer, T., Zhang, J. G., Nicola, N. A., and Norton, R. S. (1998) *J. Biol. Chem.* 273, 13738–13745.
4. Robinson, R. C., Grey, L. M., Staunton, D., Vankelecom, H., Vernallis, A. B., Moreau, J. F., Stuart, D. I., Heath, J. K., and Jones, E. Y. (1994) *Cell* 77, 1101–1116.
5. Bravo, J., and Heath, J. K. (2000) *EMBO J.* 19, 2399–2411.
6. Stewart, C. L., Kaspar, P., Brunet, L. J., Bhatt, H., Gadi, I., Kontgen, F., and Abbondanzo, S. J. (1992) *Nature* 359, 76–79.
7. Ware, C. B., Horowitz, M. C., Renshaw, B. R., Hunt, J. S., Liggitt, D., Koblar, S. A., Gliniak, B. C., McKenna, H. J., Papayannopoulou, T., Thoma, B., Cheng, L., Donovan, P. J., Peschon, J. J., Bartlett, P. F., Willis, C. R., Wright, B. D., Carpenter, M. K., Davison, B. L., and Gearing, D. P. (1995) *Development* 121, 1283–1299.

8. Vogiagis, D., and Salamonsen, L. A. (1999) *J. Endocrinol.* 160, 181–190.
9. Mitchell, M. H., Swanson, R. J., and Oehninger, S. (2002) *Biol. Reprod.* 67, 460–464.
10. Yue, Z. P., Yang, Z. M., Wei, P., Li, S. J., Wang, H. B., Tan, J. H., and Harper, M. J. (2000) *Biol. Reprod.* 63, 508–512.
11. Zwick, M. B., Shen, J., and Scott, J. K. (1998) *Curr. Opin. Biotechnol.* 9, 427–436.
12. Cochran, A. G. (2000) *Chem. Biol.* 7, R85–R94.
13. Fairlie, W. D., Uboldi, A. D., De Souza, D. P., Hemmings, G. J., Nicola, N. A., and Baca, M. (2002) *Protein Expression Purif.* 26, 171–178.
14. Nicholson, S. E., De Souza, D., Fabri, L. J., Corbin, J., Willson, T. A., Zhang, J. G., Silva, A., Asimakis, M., Farley, A., Nash, A. D., Metcalf, D., Hilton, D. J., Nicola, N. A., and Baca, M. (2000) *Proc. Natl. Acad. Sci. U.S.A.* 97, 6493–6498.
15. Hirata, Y., Kimura, N., Sato, K., Ohsugi, Y., Takasawa, S., Okamoto, H., Ishikawa, J., Kaisho, T., Ishihara, K., and Hirano, T. (1994) *FEBS Lett.* 356, 244–248.
16. Kunkel, T. A., Bebenek, K., and McClary, J. (1991) *Methods Enzymol.* 204, 125–139.
17. Sidhu, S. S., Kalmar, G. B., Willis, L. G., and Borgford, T. J. (1995) *J. Biol. Chem.* 270, 7594–7600.
18. Sidhu, S. S., Lowman, H. B., Cunningham, B. C., and Wells, J. A. (2000) *Methods Enzymol.* 328, 333–363.
19. Vieira, J., and Messing, J. (1987) *Methods Enzymol.* 153, 3–11.
20. Bitard, J., Daburon, S., Duplomb, L., Blanchard, F., Vuisio, P., Jacques, Y., Godard, A., Heath, J. K., Moreau, J. F., and Taupin, J. L. (2003) *J. Biol. Chem.* 278, 16253–16261.
21. Layton, M. J., Owczarek, C. M., Metcalf, D., Clark, R. L., Smith, D. K., Treutlein, H. R., and Nicola, N. A. (1994) *J. Biol. Chem.* 269, 29891–29896.
22. Brady, G. P., Jr., and Stouten, P. F. (2000) *J. Comput.-Aided Mol. Des.* 14, 383–401.
23. Hudson, K. R., Vernallis, A. B., and Heath, J. K. (1996) *J. Biol. Chem.* 271, 11971–11978.
24. Veronese, F. M. (2001) *Biomaterials* 22, 405–417.
25. Sidhu, S. S., Fairbrother, W. J., and Deshayes, K. (2003) *ChemBiochem.* 4, 14–25.

BI035303V